

Kinetics of the HCCO + NO₂ Reaction

Justin P. Meyer and John F. Hershberger*

Department of Chemistry and Molecular Biology, North Dakota State University, Fargo, North Dakota 58105

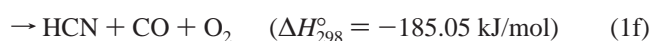
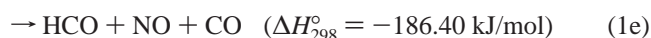
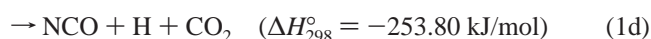
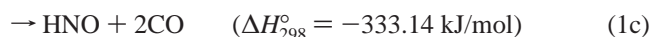
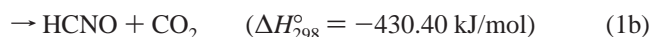
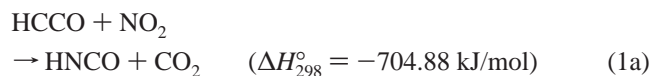
Received: February 7, 2005; In Final Form: April 1, 2005

The kinetics of the HCCO + NO₂ reaction were investigated using a laser photolysis/infrared diode laser absorption technique. Ethyl ethynyl ether (C₂H₅OCCH) was used as the HCCO radical precursor. Transient infrared detection of the HCCO radical was used to determine a total rate constant fit to the following expression: $k_1 = (2.43 \pm 0.26) \times 10^{-11} \exp[(171.1 \pm 36.9)/T] \text{ cm}^3 \text{ molecule}^{-1} \text{ s}^{-1}$ over the temperature range of 298–423 K. Transient infrared detection of CO, CO₂, and HCNO products was used to determine the following branching ratios at 298 K: $\phi(\text{HCO} + \text{NO} + \text{CO}) = 0.60 \pm 0.05$ and $\phi(\text{HCNO} + \text{CO}_2) = 0.40 \pm 0.05$.

1. Introduction

The ketylenyl radical (HCCO) is an important intermediate in hydrocarbon combustion. In particular, HCCO is formed by the oxidation of acetylene.^{1–5} Several spectroscopic^{1,2,6–10} and kinetic,^{2–5,11–22} as well as theoretical,^{11,23,24} studies of the HCCO radical have been reported. Total rate constant measurements include reactions of HCCO with NO,^{2,14,17,18} NO₂,^{18,20} O₂,^{18,21} H,^{12,22} O,^{11,16} and C₂H₂.^{18,21}

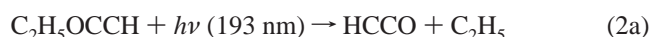
The reactions of HCCO with NO_x are of special interest, because of their evident role in NO-reburning mechanisms,^{25,26} one of the main strategies for the removal of NO_x from the combustion of fossil fuels.^{26–29} Several studies have examined the product yields of the HCCO + NO reaction, with recent data converging on HCNO + CO as the major product channel.^{13,19,23,24,30} For HCCO + NO₂, numerous product channels are thermodynamically feasible:



The thermochemistry shown was determined using data from Osborn et al.¹ for HCCO, Lin and co-workers²⁴ for HCNO, East and Allen³¹ for NCO, and NIST–JANAF³² for all other values. Two previous reports of the total rate constant for reaction 1 have appeared: Temps et al. used a discharge flow system to obtain a value of $k_1 = 2.66 \times 10^{-11} \text{ cm}^3 \text{ molecule}^{-1} \text{ s}^{-1}$ at 298 K,¹⁸ and Carl et al. used laser-photofragment/LIF to obtain a

value of $k_1 = 2.3 \times 10^{-11} \exp(340/T) \text{ cm}^3 \text{ molecule}^{-1} \text{ s}^{-1}$ over the temperature range of 293–769 K. No previous reports of the product branching of this reaction have appeared. In this paper, we report a flash photolysis/infrared absorption study of the total rate constant for reaction 1 over the temperature range of 298–423 K, along with the first reported values for the product branching for this reaction.

In the experiments reported here, we have used ethyl ethynyl ether (C₂H₅OCCH) as a photolytic precursor for HCCO radicals. The 193 nm photodissociation dynamics of this molecule has been recently studied:³³



Reaction 2a was the only observed pathway at a photolysis wavelength of 193 nm.³³ Therefore, this molecule represents a relatively clean precursor for HCCO radicals, unlike previous methods such as CH₂CO photolysis^{13,22} or the O + C₂H₂ reaction,^{18,19} which both produce large amounts of CH₂.^{4,12,27,34} The C₂H₅OCCH precursor has been used in two previous kinetic studies: a recent report on the HCCO + O₂ reaction,¹⁵ and a study done in our laboratory on the product branching ratios of HCCO + NO.³⁵

2. Experimental Section

The experimental procedure is similar to that described in previous publications.^{30,35–37} Photolysis light (with a wavelength of 193 nm) was provided by an excimer laser (Lambda Physik, Compex 200). Several lead salt diode lasers (Laser Components, Inc.) operating in the 80–110 K temperature range were used to provide tunable infrared probe laser light. Reference gases (N₂O, CO, OCS, or CO₂) were used to provide spectra for wavelength calibration of the IR light source using tabulated line positions.³⁸ The IR beam was collimated by a lens and combined with the 193 nm UV light by means of a dichroic mirror, with both beams then co-propagated through a 1.43 m absorption cell. After the UV light was removed by a second mirror, the infrared beam was passed into a 0.25 m monochromator and focused onto a 1-mm InSb detector (from Cincinatti Electronics, with a response time of ~1 μs). Transient infrared

TABLE 1: Absorption Lines Used To Probe Various Reactant Molecules

molecule	absorption line
HCCO (antisymmetric stretch)	R(17) line at 2034.8152 cm ⁻¹ , R(12) line at 2031.5931 cm ⁻¹
CO($\nu=1 \leftarrow \nu=0$)	P(14) at 2086.323 cm ⁻¹
CO ₂ (00°1) \leftarrow (00°0)	P(14) at 2337.659 cm ⁻¹
HCNO(0100°0°) \leftarrow (0000°0°)	R(10) at 2203.851 cm ⁻¹
HNCO	ν_2 band at 2268.8921 cm ⁻¹
N ₂ O(00°1) \leftarrow (00°0)	P(22) line at 2203.733 cm ⁻¹
HNO	2629–2630 cm ⁻¹

absorption signals were recorded on a digital oscilloscope (Lecroy model 9310A) and transferred to a computer for analysis. For experiments at elevated temperatures, a 1.22 m Pyrex absorption cell that was wrapped in a ceramic heat tape was used.

All of the experiments were performed on static gas mixtures. To ensure complete mixing of reagents, gases were allowed to stand for 5 min in the reaction cell. Typically, only 5–10 photolysis laser shots (at a repetition rate of 1 Hz) were signal-averaged for total rate constant experiments, and <5 shots were used for the product yield experiments. Under these conditions, only a minimal buildup of products or a depletion of reactants was observed.

Samples of SF₆ and CF₄ (Matheson) were purified by repeated freeze–pump–thaw cycles at 77 K. Traces of CO₂ were removed from SF₆ by the use of an Ascarite trap. NO₂ (Matheson) was purified by repeated freeze–pump–thaw cycles at 77 K, followed by numerous cycles at 200 K to remove traces of NO, N₂O, and CO₂. C₂H₅OCCH (50 wt % in hexane/ethanol (40/10)) samples were obtained from Aldrich and were purified by several freeze–pump–thaw cycles. A significant amount of hexane/ethanol remained in the sample after purification to stabilize the sample when not in use, as well as to dilute the vapor for more-accurate measurement of gas delivered to the reaction cell. Small quantities of hexane/ethanol in the reaction mixtures are not expected to affect the results.

Authentic HCNO samples were synthesized via the vacuum pyrolysis of 3-phenyl-4-oximino-isoxazol-5-(4H)-one, as described in the literature.^{39,40} Details of the procedure used to calibrate the HCNO absorption signals can be found in previous work.³⁵ An authentic HNCO sample was prepared via the reaction of steric acid with potassium cyanate. After purification, this sample was then used as a reference gas to locate spectral lines in the ν_2 band of HNCO, using data found in the literature.⁴¹

HCCO reactant molecules, along with CO, CO₂, HCNO, HNCO, and N₂O product molecules, were probed using the absorption lines noted in Table 1.

The HITRAN molecular database was used to locate and identify the spectral lines of CO, CO₂, and N₂O product molecules.³⁸ Other published spectral data^{2,43} were used to locate and identify HCCO and HCNO. The spectral lines used for all molecules are near the peak of the rotational Boltzmann distribution, minimizing the sensitivity to small heating effects. For CO₂ product molecule measurements, the infrared laser beam path was purged with N₂ to remove atmospheric CO₂.

The Fourier transform infrared (FT-IR) spectroscopy study was conducted using a Nexus 470 FT-IR system (Thermo Nicolet) at a resolution of 0.5 cm⁻¹ using an 11-cm Pyrex gas cell.

3. Results

3.1. Total Rate Constants. When photolysis of the C₂H₅-OCCH/NO₂/SF₆ mixtures was performed, a transient absorption

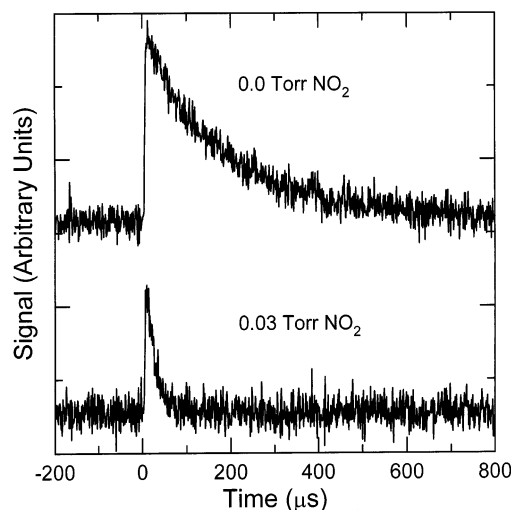


Figure 1. HCCO transient signals at different partial pressures of NO₂. Reaction conditions: $P_{\text{C}_2\text{H}_5\text{OCCH}} = 0.05$ Torr, $P_{\text{SF}_6} = 1.0$ Torr, and, for the lower trace, $P_{\text{NO}_2} = 0.03$ Torr.

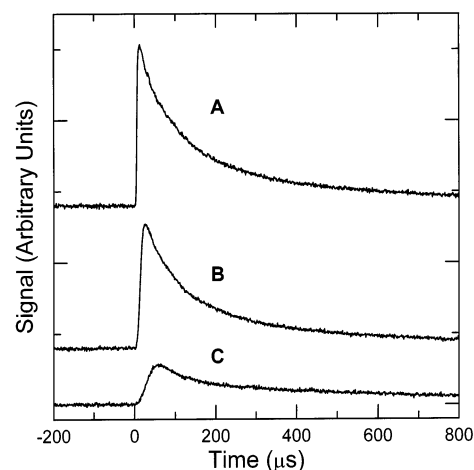


Figure 2. HCCO transient signals observed with varied SF₆ pressures at 2031.5931 cm⁻¹. Reaction conditions: $P_{\text{C}_2\text{H}_5\text{OCCH}} = 0.05$ Torr, $P_{\text{SF}_6} = 1.0$ Torr (trace A), $P_{\text{SF}_6} = 0.2$ Torr (trace B), $P_{\text{SF}_6} = 0.0$ Torr (trace C), $T = 298$ K.

was observed at 2034.8152 cm⁻¹, corresponding to the R(17) rotational transition of the antisymmetric stretch of HCCO (the R(12) rotational transition was also used).² Using typical photolysis laser energies of ~2–3 mJ/pulse, transient absorptions of <5% of the probe laser intensity were observed. Small off-resonant background transients (<10% of the on-resonant transient) were observed when the probe laser was detuned ~0.02 cm⁻¹ off the HCCO line. These background signals, which are attributed to thermal deflection of the probe laser, were subtracted from the on-resonant signals to obtain HCCO time-resolved absorption profiles. A typical HCCO absorption profile is shown in Figure 1. These signals display a fast rise, followed by a slower decay, which is consistent with rapid HCCO production by photolysis of the C₂H₅OCCH precursor, followed by the removal of HCCO by reactions or diffusion out of the beam path.

The HCCO signals were determined to be dependent significantly on the SF₆ pressure, as shown in Figure 2. Most notably, the signals collected without SF₆ display a very long rise time. These data suggest that (i) HCCO radicals are produced with substantial vibration excitation, and (ii) SF₆ buffer gas is effective in relaxing the nascent vibrational distribution to a Boltzmann distribution.

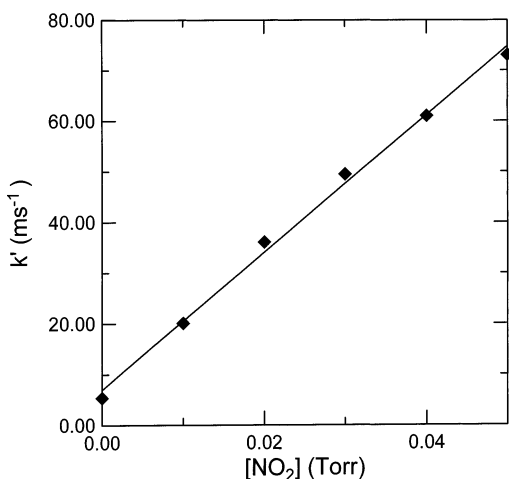


Figure 3. Pseudo-first-order decay rate constant of the HCCO radical, as a function of NO₂ pressure, using the HCCO R(17) line at 2034.815 cm⁻¹. Reaction conditions: $P_{\text{C}_2\text{H}_5\text{OCCH}} = 0.05$ Torr, $P_{\text{SF}_6} = 1.0$ Torr, and $P_{\text{NO}_2} = \text{variable}$, $T = 298$ K.

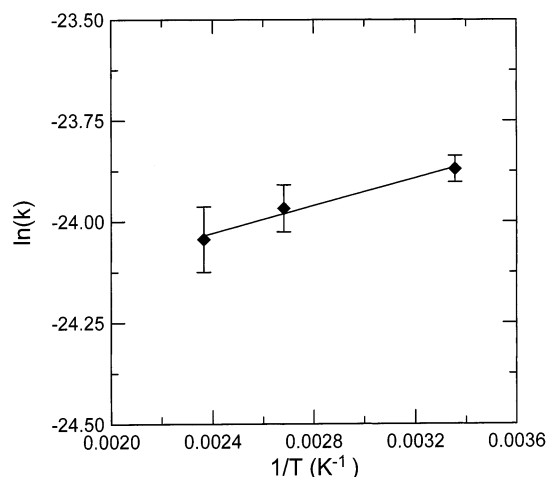


Figure 4. Arrhenius plot for the HCCO + NO₂ reaction over the temperature range of 298–423 K.

Typical reaction conditions were 0.050 Torr for the C₂H₅OCCH precursor, 0.00–0.060 Torr for the NO₂, and 1.0 Torr for the SF₆ buffer gas. Under these conditions, at typical photolysis laser pulse energies, we estimate an upper limit for the HCCO radical density of $\sim 2.0 \times 10^{13}$ molecules/cm³. Therefore, pseudo-first-order conditions of [HCCO] \ll [NO₂] were met whenever a NO₂ reagent was included.

The transient decays were fit to single exponential decays to obtain pseudo-first-order rate constants (k'). Figure 3 shows a plot of k' versus the NO₂ pressure. As per standard kinetic treatments, the slope of these plots gives the desired second-order rate constant k_1 . The nonzero intercept in Figure 3 is due to HCCO + HCCO self-reactions and/or reactions with other fragments or radicals formed by photolysis of the C₂H₅OCCH precursor, as well as diffusion of HCCO out of the probe beam path. At the pressure and beam geometries used, diffusion occurs on a ~ 1 ms time scale, which is slower than the observed decays. Therefore, diffusion does not significantly affect the transient signal. Experiments were conducted over the temperature range of 298–423 K. The upper temperature limit on the measurements is due to the apparent thermal dissociation of the ethyl ethynyl ether precursor, which results in negligible HCCO transient signals at higher temperatures. Figure 4 shows an Arrhenius plot of the data. The data were fit to the following Arrhenius expression (error bars represent one

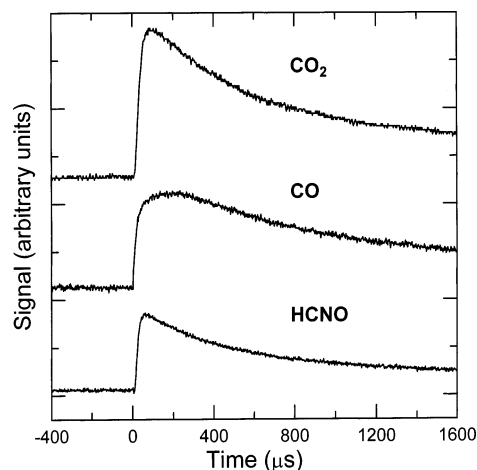


Figure 5. Transient infrared absorption signals of CO₂, CO, and HCNO product molecules. Reaction conditions: $P_{\text{C}_2\text{H}_5\text{OCCH}} = 0.02$ Torr, $P_{\text{NO}_2} = 0.05$ Torr, and $P_{\text{SF}_6} = 0.8$ Torr. For the CO signal, $P_{\text{CF}_4} = 0.8$ Torr was also added.

standard deviation):

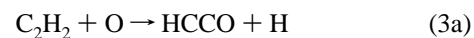
$$k_1(\text{cm}^3 \text{ molecule}^{-1} \text{ s}^{-1}) = (2.43 \pm 0.26) \times 10^{-11} \exp\left(\frac{171.1 \pm 36.9}{T}\right)$$

3.2. Product Channels. Transient infrared laser absorption was used to attempt detection of the following product molecules: HNCO, HCNO, CO₂, N₂O, and CO. No transient signals for HNCO or N₂O were detected. All product detection experiments were conducted at 298 K.

Large transient signals for three of these molecules—HCNO, CO₂, and CO—were observed, as shown in Figure 5. Identical partial pressures of C₂H₅OCCH, NO₂, and SF₆ were used for detection of each molecule, with one exception. CF₄ was included as an additional buffer gas for the detection of CO, because of the fact that it has been shown to relax vibrationally excited CO more efficiently than SF₆. These signals display a prompt rise in absorption, followed by a slow decay. The decay is due to diffusion of product species out of the probed volume. The peak amplitudes of the transients for CO and CO₂ were then converted to absolute concentrations, using published lines strengths³⁸ and equations that have been described previously.⁴⁴ HCNO concentrations were determined in a similar manner; however, a previously determined absorption coefficient calibration from an authentic HCNO sample was used.³⁵ In some cases, small corrections to the product yields were made, to account for the variations in photolysis laser energy during an experimental run.

4. Discussion

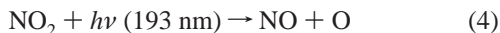
4.1. Total Rate Constant. There are two previous measurements of the rate constant of the HCCO + NO₂ reaction. Temps et al. used the O + C₂H₂ reaction to form HCCO radicals:¹⁸



They obtained a value of $k_1 = 2.66 \times 10^{-11}$ cm³ molecule⁻¹ s⁻¹ at 298 K. Carl and co-workers used the photolysis of ketene to produce HCCO and reported a rate constant of 7.2×10^{-11} cm³ molecule⁻¹ s⁻¹ at 298 K. Both of these approaches have potential complications from the formation of significant

amounts of CH₂ radicals. Our data indicate a value of $k_1 = 4.31 \times 10^{-11} \text{ cm}^3 \text{ molecule}^{-1} \text{ s}^{-1}$ at 298 K, which is between the two previous reported values. Recent studies have shown that the ethyl ethynyl ether used in our experiments is a relatively clean HCCO precursor at 193 nm.³³ This observation has a tendency to minimize the secondary chemistry that arises from other radical species.

NO₂ is known to dissociate at 193 nm:



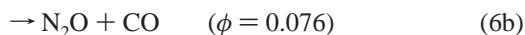
This would lead to the formation of NO in the reaction cell, as well as a loss of 193 nm in photolysis energy (causing lower concentrations of HCCO to be produced). An absorption coefficient measurement at 193 nm for NO₂ resulted in $\alpha = 0.0277 \text{ Torr}^{-1} \text{ cm}^{-1}$. Calculations using this absorption coefficient and an average laser pulse energy of 2 mJ predict a <1% conversion of NO₂ into NO and O. Under these conditions, virtually all of the HCCO radicals formed will therefore react with NO₂, and the effects of dissociation of NO₂ are negligible.

4.2. Product Channels. Attempts to detect N₂O or HNCO were unsuccessful. In fact, even after multiple (~100) photolysis laser pulses, no static absorption for these species was observed. The failure to observe HNCO indicates that reaction 1a is, at most, a minor channel, although the lack of HNCO line strength information prevents us from making a quantitative estimate for an upper limit of ϕ_{1a} .

Our failure to observe N₂O allows us to eliminate channels 1d, 1g, and 1h. Channels 1d and 1g can be eliminated, because the reaction of NCO with NO₂ is expected to form N₂O in high yield:⁴⁵



Channel 1h can also be eliminated because CN would react with excess NO₂ to form NCO in high yield via reaction 6, which would proceed to form N₂O by reaction 5:⁴⁶

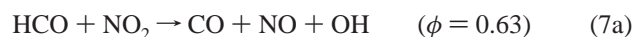


We estimate an upper limit of 0.01 for the production of N₂O via these channels.

In principle, HCN production is possible through channel 1f. The HCN absorption band near 3310 cm⁻¹ lies outside the range of our available diode lasers.³² Therefore, an FT-IR study was performed using a typical fill of C₂H₅OCCH/SF₆/NO₂ from the 1.43-m Pyrex reaction cell that was transferred to a 0.11-m Pyrex gas cell for use in an FT-IR study. A duplicate fill of C₂H₅OCCH/SF₆/NO₂ was then exposed to >1000 193-nm laser pulses with an average pulse energy of ~0.3 mJ (measured by a detector placed after the reaction cell). The resulting gas mixture was then transferred to the same 0.11-m Pyrex gas cell. A subtraction of the two FT-IR spectra was observed to show the production of CO₂, NO, HCNO, and CO. No evidence of HCN was observed in the FT-IR spectra. This is evidence that product channel 1f is likely a minor channel as well. In addition, no evidence of *trans*-HONO was observed in the FT-IR analysis near 1263 cm⁻¹.⁴⁷ Additional evidence for the lack of significant contribution of channels 1i and 1j is that the CCO + NO₂ reaction would likely produce NCO as a significant product channel (although no literature data exist to prove this), resulting in N₂O formation via reaction 5. The ability to quantify an upper limit was not possible using FT-IR; therefore, values for upper limits of ϕ_{1f} , ϕ_{1i} , or ϕ_{1j} could not be determined.

An attempt was made using transient absorption to observe HNO products in the range of 2629–2630 cm⁻¹, using published line positions for the ν_1 transitions for HNO.⁴³ No transient signals were found in the 2629–2630 cm⁻¹ wavelength range, which includes three recorded spectral lines.⁴³ Little is known about the kinetics of HNO; however, a review suggests a very slow rate constant for the HNO + NO₂ reaction ($k = 3.57 \times 10^{-14}$ at 300 K).⁴⁸ We conclude that channel 1c is likely not a major channel; however, the lack of published line strengths prevents a quantitative estimate of an upper limit for reaction channel 1c.

Therefore, the major channels for reaction 1 were concluded to be pathways 1b and 1e. Any HCO produced in channel 1e would react with the excess NO₂, producing additional CO and CO₂ in branching ratios of $\phi = 0.63$ and 0.37, respectively:³⁶



The total concentration of key products can be found using the following equations:

$$[\text{HCNO}]_{\text{Tot}} = [\text{HCNO}]_{1b} \quad (8)$$

$$[\text{CO}_2]_{\text{Tot}} = [\text{CO}_2]_{1b} + [\text{CO}_2]_{7b} \quad (9)$$

$$[\text{CO}]_{\text{Tot}} = [\text{CO}]_{1e} + [\text{CO}]_{7a} \quad (10)$$

$$[\text{HCO}]_{\text{Tot}} = [\text{HCO}]_{1e} \quad (11)$$

The $[\text{HCNO}]_{\text{Tot}}$, $[\text{CO}_2]_{\text{Tot}}$, and $[\text{CO}]_{\text{Tot}}$ values are obtained directly from the product yield measurement; thus, the $[\text{HCO}]_{\text{Tot}}$ value (HCO produced in the initial reaction) could be determined using two different methods, as follows. Each method assumes total consumption of HCCO and HCO by reaction with excess NO₂. The first method is based on measurement of the excess of the CO₂ concentration, compared to the measured HCNO concentration:

$$[\text{HCO}]_{\text{Tot}} = \frac{[\text{CO}_2]_{\text{Tot}} - [\text{HCNO}]_{\text{Tot}}}{0.37} \quad (12)$$

The second method obtains the HCO yield from the CO signals:

$$[\text{HCO}]_{\text{Tot}} = \frac{[\text{CO}]_{\text{Tot}}}{1.63} \quad (13)$$

Branching ratios for product channels 1b and 1e can then be found by comparing the HCNO concentrations with HCO concentrations that have been determined using both eqs 12 and 13, as shown in Table 2.

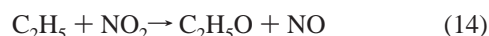
Problems that result from the methods for determination of HCO concentration can be observed in Table 2. Ideally, the HCO concentration calculated from eq 12 should match that of eq 13. This is not the case for many experimental runs from Table 2. This discrepancy arises primarily because the $[\text{CO}_2]_{\text{Tot}}$ and $[\text{HCNO}]_{\text{Tot}}$ yields are similar in magnitude, resulting in significant random error when the subtraction in eq 12 is performed. This is probably the reason the greater standard deviation is observed for the calculation using eq 12. In addition, eq 12 is subject to potential systematic errors that result from uncertainties in the calibration of HCNO yields. For this reason,

TABLE 2: Product Yield Data

run	Product Yields ($\times 10^{12}$ molecules/cm ³)					Branching Ratio, ϕ			
	Experimental		Calculated (eq 12)	Calculated (eq 13)		Calculated Using eq 12		Calculated Using eq 13	
	HCNO	CO ₂	CO	[HCO]	[HCO]	Φ_{1b}	Φ_{1e}	Φ_{1b}	Φ_{1e}
1	1.317	2.153	3.225	2.259	1.979	0.37	0.63	0.40	0.60
2	2.350	2.748	5.264	1.076	3.229	0.69	0.31	0.42	0.58
3	1.526	1.972	3.016	1.205	1.850	0.56	0.44	0.45	0.55
4	1.477	2.072	2.945	1.608	1.807	0.48	0.52	0.45	0.55
5	1.260	2.236	4.362	2.638	2.676	0.32	0.68	0.32	0.68
6	2.437	3.217	6.622	2.108	4.063	0.54	0.46	0.37	0.63
7	0.857	1.389	2.469	1.438	1.515	0.37	0.63	0.36	0.64
				average:		0.47 ± 0.13	0.53 ± 0.13	0.40 ± 0.05	0.60 ± 0.05

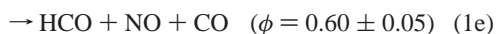
branching ratios that have been determined using eq 13 were viewed as more reliable and used for the final branching values, although it should be noted that branching ratios determined using both methods were fairly similar.

Detection of NO products was not attempted for multiple reasons. First, NO production is expected from NO₂ photolysis (reaction). Furthermore, the photolysis of C₂H₅OCCH produces ethyl radicals (C₂H₅), which are expected to react with NO₂, producing NO:



The total rate constant for reaction 14 has been reported to be $k_{14} = 4.5 \times 10^{-11} \text{ cm}^3 \text{ molecule}^{-1} \text{ s}^{-1}$.⁴⁹ This reaction is expected to form sufficient quantities of NO, to prevent us from quantifying the NO production from reaction 1.

By averaging all the branching ratios calculated using eq 13, the following branching ratios were determined (uncertainties represent one standard deviation):



5. Conclusions

The HCCO + NO₂ reaction has been studied using the ethyl ethynyl ether precursor for HCCO formation. The total rate constant was determined over the temperature range of 298–423 K and fit to the following rate expression: $k_1 = (2.43 \pm 0.26) \times 10^{-11} \exp[(171.1 \pm 36.9)/T] \text{ cm}^3 \text{ molecule}^{-1} \text{ s}^{-1}$. The detection of CO, CO₂, and HCNO products yielded the following branching ratios at 298 K: $\phi_{1e}(\text{HCO} + \text{NO} + \text{CO}) = 0.60 \pm 0.05$ and $\phi_{1b}(\text{HCNO} + \text{CO}_2) = 0.40 \pm 0.05$.

Acknowledgment. This work was supported by the Division of Chemical Sciences, Office of Basic Energy Sciences of the Department of Energy (under Grant No. DE-FG03-96ER14645).

References and Notes

- Osborn, D. L.; Mordaunt, D. H.; Choi, H.; Bise, R. T.; Neumark, D. M.; Rohlfling, C. M. *J. Chem. Phys.* **1997**, *106*, 10087.
- Unfried, K. G.; Glass, G. P.; Curl, R. F. *Chem. Phys. Lett.* **1991**, *177*, 33.
- Michael, J. V.; Wagner, A. F. *J. Phys. Chem.* **1990**, *94*, 2453.
- Williamson, D. G.; Bayes, K. D. *J. Phys. Chem.* **1969**, *73*, 1232.
- Schmoltner, A. M.; Chu, P. M.; Lee, Y. T. *J. Chem. Phys.* **1989**, *91*, 5365.
- Mordaunt, D. H.; Osborn, D. L.; Choi, H.; Bise, R. T.; Neumark, D. M. *J. Chem. Phys.* **1996**, *105*, 6078.
- Endo, Y.; Hirota, E. *J. Chem. Phys.* **1987**, *88*, 4319.
- Brock, L. R.; Mischler, B.; Rohlfling, E. A. *J. Chem. Phys.* **1997**, *107*, 665.
- Brock, L. R.; Mischler, B.; Rohlfling, E. A. *J. Chem. Phys.* **1999**, *110*, 6773.
- Unfried, K. G.; Curl, R. F. *J. Mol. Spectrosc.* **1991**, *150*, 86.
- Peeters, J.; Langhans, I.; Boullart, W.; Nguyen, M. T.; Devriendt, K. *J. Phys. Chem.* **1994**, *98*, 11988.
- Vinckier, C.; Schaekers, M.; Peeters, J. *J. Phys. Chem.* **1985**, *89*, 508.
- Rim, K. T.; Hershberger, J. F. *J. Phys. Chem. A* **2000**, *104*, 293.
- Carl, S. A.; Sun, Q.; Vereecken, L.; Peeters, J. *J. Phys. Chem.* **2002**, *106*, 12242.
- Osborn, D. L. *J. Phys. Chem. A* **2003**, *107*, 3728.
- Peeters, J.; Boullart, W.; Devriendt, K. *J. Phys. Chem.* **1995**, *99*, 3583.
- Boullart, W.; Nguyen, M. T.; Peeters, J. *J. Phys. Chem.* **1994**, *98*, 8036.
- Temps, F.; Wagner, H. G.; Wolf, M. Z. *Phys. Chem. (Muenchen, Ger.)* **1992**, *176*, 27.
- Eickhoff, U.; Temps, F. *Phys. Chem. Chem. Phys.* **1999**, *1*, 243.
- Carl, S. A.; Sun, Q.; Teugels, L.; Peeters, J. *Phys. Chem. Chem. Phys.* **2003**, *5*, 5424.
- Murray, K. K.; Unfried, K. G.; Glass, G. P.; Curl, R. F. *Chem. Phys. Lett.* **1992**, *192*, 512.
- Glass, G. P.; Kumaran, S. S.; Michael, J. V. *J. Phys. Chem. A* **2000**, *104*, 8360.
- Vereecken, L.; Sumathy, R.; Carl, S. A.; Peeters, J. *Chem. Phys. Lett.* **2001**, *344*, 400.
- Tokmakov, I. V.; Moskaleva, L. V.; Paschenko, D. V.; Lin, M. C. *J. Phys. Chem. A* **2003**, *107*, 1066.
- Miller, J. A.; Bowman, C. T. *Prog. Energy Combust. Sci.* **1989**, *15*, 287.
- Glarborg, P.; Alzueta, M. U.; Dam-Johansen, K.; Miller, J. A. *Combust. Flame* **1998**, *115*, 1.
- Eshchenko, G.; Kocher, T.; Kerst, C.; Temps, F. *Chem. Phys. Lett.* **2002**, *356*, 181.
- Miller, J. A.; Durant, J. L.; Glarborg, P. *Symp. (Int.) Combust. Proc.* **1998**, *27*, 235.
- Jones, J. C. *Combustion Science: Principles and Practice*; Millennium Books: Newtown, Australia, 1993.
- Meyer, J. P.; Hershberger, J. F. *J. Phys. Chem. A*, in press. (George W. Flynn Festschrift.)
- East, A. L. L.; Allen, W. D. *J. Chem. Phys.* **1993**, *99*, 4638.
- Chase, M. W. NIST–JANAF Thermochemical Tables. *J. Phys. Chem. Ref. Data*, 1998; Vol. 4th ed.
- Kirsch, M. J.; Miller, J. L.; Butler, L. J.; Su, H.; Bersohn, R.; Shu, J. *J. Chem. Phys.* **2003**, *119*, 176.
- Schmoltner, A. M.; Chu, P. M.; Lee, Y. T. *J. Chem. Phys.* **1989**, *91*, 5365.
- Cooper, W. F.; Hershberger, J. F. *J. Phys. Chem.* **1992**, *96*, 771.
- Rim, K. T.; Hershberger, J. F. *J. Phys. Chem. A* **1998**, *102*, 5898.
- Thweatt, W. D.; Erickson, M. A.; Hershberger, J. F. *J. Phys. Chem. A* **2004**, *108*, 74.
- Rothman, L. S. *J. Quant. Spectrosc. Radiat. Transfer* **1992**, *48*, 469.
- Pasinszki, T.; Kishimoto, N.; Ohno, K. *J. Phys. Chem.* **1999**, *103*, 6746.
- Wentrup, C.; Gerecht, B.; Briehl, H. *Angew. Chem., Int. Ed. Engl.* **1979**, *18*, 467.
- Lemoine, B.; Yamada, K.; Winnewisser, G. *Ber. Bunsen-Ges.* **1982**, *86*, 795.
- Ferretti, E. L.; Rao, K. N. *J. Mol. Spectrosc.* **1974**, *51*, 97.
- Johns, J. W. C.; McKellar, A. R. W.; Weinberger, E. *Can. J. Phys.* **1983**, *61*, 1106.
- Cooper, W. F.; Park, J.; Hershberger, J. F. *J. Phys. Chem.* **1993**, *97*, 3283.
- Park, J.; Hershberger, J. F. *J. Phys. Chem.* **1993**, *97*, 13647.
- Park, J.; Hershberger, J. F. *J. Chem. Phys.* **1993**, *99*, 3488.
- Ramazan, K. A.; Syomin, D.; Finlayson-Pitts, B. J. *Phys. Chem. Chem. Phys.* **2004**, *6*, 3836.
- Tsang, W.; Herron, J. T. *J. Phys. Chem. Ref. Data* **1991**, *20*, 609.
- Park, J.-Y.; Gutman, D. *J. Phys. Chem.* **1983**, *87*, 1844.